



Article

Comparison of Pharmacokinetics and Anti-Pulmonary Fibrosis-Related Effects of Sulforaphane and Sulforaphane *N*-acetylcysteine

Eun Suk Son ^{1,†}, Xiang Fei ^{2,†}, Jin-Ha Yoon ², Seung-Yong Seo ², Han-Joo Maeng ², Sung Hwan Jeong ^{1,*} and Yu Chul Kim ^{3,4,*}

¹ Department of Medicine, Gachon University Gil Medical Center, Incheon 21565, Korea; eunsuk0607@hanmail.net

² Department of Pharmacy, College of Pharmacy, Gachon University, Incheon 21936, Korea; mrfeixiang@gmail.com (X.F.); jinha89@daum.net (J.-H.Y.); syseo@gachon.ac.kr (S.-Y.S.); hjmaeng@gachon.ac.kr (H.-J.M.)

³ Department of Pharmaceutical Engineering, Inje University, Gimhae 50834, Korea

⁴ Institute of Digital Anti-Aging Healthcare, Inje University, Gimhae 50834, Korea

* Correspondence: jsw@gilhospital.com (S.H.J.); yckim@inje.ac.kr (Y.C.K.); Tel.: +82-32-458-2872 (S.H.J.); +82-55-320-3399 (Y.C.K.)

† These authors contributed equally to this work.



Citation: Son, E.S.; Fei, X.; Yoon, J.-H.; Seo, S.-Y.; Maeng, H.-J.; Jeong, S.H.; Kim, Y.C. Comparison of Pharmacokinetics and Anti-Pulmonary Fibrosis-Related Effects of Sulforaphane and Sulforaphane *N*-acetylcysteine. *Pharmaceutics* **2021**, *13*, 958. <https://doi.org/10.3390/pharmaceutics13070958>

Academic Editor: Patrick J. Sinko

Received: 30 May 2021

Accepted: 22 June 2021

Published: 25 June 2021

Publisher's Note: MDPI stays neutral with regard to jurisdictional claims in published maps and institutional affiliations.



Copyright: © 2021 by the authors. Licensee MDPI, Basel, Switzerland. This article is an open access article distributed under the terms and conditions of the Creative Commons Attribution (CC BY) license (<https://creativecommons.org/licenses/by/4.0/>).

Abstract: Sulforaphane (SFN), belonging to the isothiocyanate family, has received attention owing to its beneficial activities, including chemopreventive and antifibrotic effects. As sulforaphane *N*-acetylcysteine (SFN-NAC), a major sulforaphane metabolite, has presented similar pharmacological activities to those of SFN, it is crucial to simultaneously analyze the pharmacokinetics and activities of SFN and SFN-NAC, to comprehensively elucidate the efficacy of SFN-containing products. Accordingly, the anti-pulmonary fibrotic effects of SFN and SFN-NAC were assessed, with simultaneous evaluation of permeability, metabolic stability, and in vivo pharmacokinetics. Both SFN and SFN-NAC decreased the levels of transforming growth factor- β 1-induced fibronectin, alpha-smooth muscle actin, and collagen, which are major mediators of fibrosis, in MRC-5 fibroblast cells. Regarding pharmacokinetics, SFN and SFN-NAC were metabolically unstable, especially in the plasma. SFN-NAC degraded considerably faster than SFN in plasma, with SFN being formed from SFN-NAC. In rats, SFN and SFN-NAC showed a similar clearance when administered intravenously; however, SFN showed markedly superior absorption when administered orally. Although the plasma SFN-NAC concentration was low owing to poor absorption following oral administration, SFN-NAC was converted to SFN in vivo, as in plasma. Collectively, these data suggest that SFN-NAC could benefit a prodrug formulation strategy, possibly avoiding the gastrointestinal side effects of SFN, and with improved SFN-NAC absorption.

Keywords: sulforaphane; sulforaphane *N*-acetylcysteine; anti-pulmonary fibrosis effect; pharmacokinetics; metabolic stability

1. Introduction

Pulmonary fibrosis (PF) is pathologically characterized by accumulation of fibroblastic foci, excessive matrix deposition, and aberrant remodeling that result in impaired gas exchange, diminished lung capacity, and eventually death [1,2]. Fibroblasts, the major mesenchymal cells in the lung, are activated by fibrogenic growth factors such as tissue growth factor and transforming growth factor (TGF)- β 1, which promotes differentiation into myofibroblasts. Furthermore, myofibroblast activation induces excessive accumulation of ECM components, which destroy the alveolar structure [3,4].

Isothiocyanates are sulfur-containing phytochemicals with the general formula R-N=C=S. Sulforaphane (1-isothiocyanato-4-methylsulfinylbutane; SFN), known to belong

to this group of chemicals, is mainly present in broccoli as a glucosinolate conjugate. On the crushing and chewing of vegetables, the glucosinolate precursor of SFN is metabolized to SFN via enzymatic hydrolysis by myrosinase [5]. Previously, several studies have shown that SFN mediates chemopreventive effects by blocking the initiation of carcinogenesis, mediated by inhibiting enzymes that convert procarcinogens to carcinogens and inducing phase II enzymes that conjugate carcinogens and facilitate their excretion from the body [6,7]. Furthermore, SFN has shown direct anticancer effects by inhibiting proliferation and inducing apoptosis in tumor cell lines and animal models [8–11]. More recently, it was observed that SFN treatment attenuated the transforming growth factor (TGF)-beta1-induced expression of fibrosis-related proteins, including fibronectin (FN), type I collagen (COL1A1), type IV collagen (COL4A1), and alpha-smooth muscle actin (α -SMA) in the lung-derived cells A549 and MRC-5, in vitro [12]. Moreover, bleomycin-induced fibrosis was reportedly reduced in a mouse model following SFN treatment [12]. Following absorption, SFN is conjugated with glutathione and further metabolized to sulforaphane-cysteine, sulforaphane-cysteine-glycine, and sulforaphane *N*-acetylcysteine (SFN-NAC) [13,14]. SFN conjugates are converted to their parent form to attain an equilibrium state under physiological conditions and could be considered prodrugs of SFN. Among known SFN conjugates, SFN-NAC is the most stable conjugate and the primary form excreted in urine [15,16]. Furthermore, it has been reported that SFN-NAC has chemopreventive and anticancer activities, although SFN-NAC is a phase II enzyme-mediated metabolite [17–19]. Therefore, the pharmacokinetics of both SFN and SFN-NAC should be simultaneously investigated to clarify the pharmacological effects of SFN in terms of its antifibrotic effects.

Several studies have reported the pharmacokinetics of SFN [20–22]. SFN is well absorbed in the intestine, with an absolute bioavailability of approximately 82% at 0.5 mg/kg; however, the bioavailability decreases as the dose increases to 5 mg/kg, suggesting non-linear pharmacokinetics in rats [21]. However, the pharmacokinetics of SFN are highly variable and inconsistent in previous reports. For example, the plasma concentration profiles of SFN are highly variable between studies, and the half-life of SFN ranged between 7.6 and 65.6 h after intravenous administration in rats [21,22]. Moreover, to the best of our knowledge, the pharmacokinetics of SFN-NAC has not yet been independently evaluated. The non-linear pharmacokinetics and high variability in pharmacokinetic parameters of SFN could induce inter-subject variability for the pharmacological effects of SFN and SFN-NAC. In the present study, we compared the in vitro anti-pulmonary fibrosis effects of SFN and SFN-NAC using human lung fibroblast cells (MRC-5). In addition, the pharmacokinetics of SFN in the micro-dose range, which seemed to follow linear kinetics, was investigated. In addition, the pharmacokinetics of SFN-NAC, an active metabolite of SFN, was evaluated along with the formed SFN.

2. Materials and Methods

2.1. Chemicals and Reagents

The structures of SFN and SFN-NAC are shown in Figure 1. SFN (cat. # S699115) and SFN-NAC (cat. # S699120) were purchased from TRC (North York, ON, Canada). Human and rat plasma were obtained from XenoTech (Kansas City, KS, USA). Human and rat liver microsomes were purchased from BD Biosciences (Corning, NY, USA), and water was purified using the aquaMAX™ ultra-pure water purification system (YL Instruments, Anyang, Korea). All other chemicals and solvents were of reagent or HPLC grade and were used without further purification.

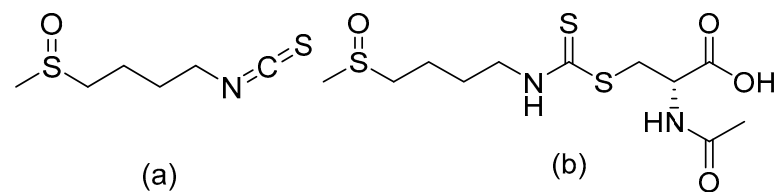


Figure 1. Chemical structures of (a) Sulforaphane (SFN) and (b) Sulforaphane *N*-acetylcysteine (SFN-NAC).

2.2. *In Vitro* Anti-Lung Fibrosis Effects

2.2.1. Cell Viability Assay

Human lung fibroblast cells (MRC-5) were purchased from the Korean Cell Line Bank and cultured in Dulbecco's modified Eagle's medium (WelGene, Gyeongsan, Korea) supplemented with 100 µg/mL streptomycin (WelGene), 100 U/mL penicillin (WelGene), and 10% fetal bovine serum (WelGene). Then, cells were treated with different concentrations of SFN (10 and 20 µM) and SFN-NAC (10 and 20 µM) for the indicated time periods. The cells were also treated with 0.1% dimethyl sulfoxide (DMSO) as a vehicle control.

In brief, cells were seeded into 96-well plates and exposed to various concentrations of SFN and SFN-NAC for 24–72 h prior to the addition of 10 µL MTT solution (3-(4,5-dimethylthiazol-2-yl)-2,5-diphenyltetrazolium bromide; 5 mg/mL in DPBS) to each well. After 4 h of incubation at 37 °C, the medium was gently removed, and 100 µL DMSO was added. The absorbance was measured at 550 nm using a microplate reader (Thermo LabSystems, Helsinki, Finland).

2.2.2. Quantitative Reverse Transcription-PCR (qRT-PCR) Analysis

Total RNA was extracted using RNAiso Plus reagent (Takara Bio, Shiga, Japan), and cDNA was synthesized from total RNA using a Prime Script RT reagent kit (Takara Bio). qRT-PCR reactions were performed using a SYBR Premix kit (Takara Bio) and run on a CFX96 detection system (BioRad, Hercules, CA, USA). GAPDH was used as an internal control, and all experiments were performed in triplicate. The expression levels were calculated from the PCR profiles of each sample using the threshold cycle (Ct), corresponding to the cycle with a statistically significant increase in fluorescence. The Ct values for the endogenous control (GAPDH) were subtracted from those of the corresponding sample to correct for differences in the amount of total cDNA in the starting reaction.

The primers used for qRT-PCR were as follows: 5'-CCATCGCAAACCGCTGCCAT-3' (FN-F) and 5'-AACTTCTCAGCTATGGGCTT-3' (FN-R); 5'-ACTGAGCGTGGCTATTCC TCCGTT-3' (α-SMA-F) and 5'-GCAGTGGCCATCTCATTTC-3' (α-SMA-R); 5'-TGGCCA AGAAGACATCCCTGAAGT-3' (COL1A1-F) and 5'-ACATCAGGTTTCCACGCTCACCA-3' (COL1A1-R); 5'-TGTGGGCCAGCCAGGCATTG-3' (COL4A1-F) and 5'-CAGGGGTCC GATCGCTCCA-3' (COL4A1-R); 5'-TTGGTATCGTGGAAGGACTCA-3' (GAPDH-F) 5'-TGTCATCATATTGGCAGGTTT-3' (GAPDH-R).

2.2.3. Western Blot Analysis

In brief, cells were lysed in radioimmunoprecipitation assay (RIPA) buffer (150 mM NaCl, 50 mM Tris-HCl at pH 8.0, 0.1% SDS, 0.5% deoxycholate, 1% NP-40) with 1X protease inhibitors. Protein concentration was determined using a Pierce BCA protein assay (Thermo Fisher Scientific, Rockford, IL, USA). Then, protein was separated by 8–10% sodium dodecyl sulfate-polyacrylamide gel electrophoresis and transferred to a PVDF membrane (Millipore, Bedford, MA, USA). After blocking with 5% non-fat milk, the membrane was incubated with primary antibodies. The primary antibodies used were anti-fibronectin (Santa Cruz Biotechnology, Santa Cruz, CA, USA, sc-8422, 1:1000), anti-type 1 collagen (COL1A1) (Abcam, Cambridge, UK, ab90395, 1:1000), anti-type 4 collagen (COL4A1) (Abcam, ab135802, 1:1000), anti-alpha-SMA (Abcam, ab5694, 1:1000), and anti-GAPDH (Abfrontier, Seoul, Korea, LF-PA0018, 1:2000). The membrane was washed and then

incubated with horseradish peroxidase (HRP)-conjugated anti-mouse (Genetex, Hsinchu, Taiwan, GTX213110-01) or anti-rabbit secondary antibodies (Genetex, GTX213111-01). Antibody-bound protein was detected using a Western BLoT Hyper HRP Substrate kit (Takara Bio, Shiga, Japan). Band intensities were normalized to those of GAPDH using the ImageJ software (National Institutes of Health, Bethesda, MD, USA). All experiments were independently performed four times.

2.3. *In Vitro* Pharmacokinetic Study

2.3.1. Plasma Stability Assay

The stability of SFN and SFN-NAC was investigated in human and rat plasma. Test compounds (1 μ M) were incubated with rat and human plasma. The amount remaining (%) was determined at 0, 15, 30, 60, 120, 180, and 240 min using liquid chromatography-tandem mass spectrometry (LC-MS/MS).

2.3.2. Liver Microsomal Metabolic Stability

The metabolic stability of SFN and SFN-NAC was evaluated in human and rat liver microsomes as previously reported [23], with minor modifications. Briefly, test compounds (1 μ M) were incubated with rat and human liver microsomes (final concentration 1 mg/mL protein) containing 1 mM NADPH. The amount remaining was determined at 0, 15, 30, 60, 120, 180, and 240 min using LC-MS/MS.

2.3.3. Apparent Permeability for Direction of Absorption in Caco-2 Cells

Apparent permeability in the direction of absorption (apical-to-basolateral side) was determined as previously reported [24]. Briefly, test compounds (54 μ M) were loaded on the apical side of the Caco-2 cell monolayer, which was cultured in a transwell plate for 21 days after seeding cells at a density of 8×10^4 cells/cm². Next, to measure the absorptive transport of drugs, the inserts were moved to a well containing fresh transport media, replaced every 30 min for 2 h. The cumulative amount on the basolateral side was calculated following sample analysis using LC-MS/MS. Finally, the apparent permeability of the apical-to-basolateral side was calculated by dQ/dt , the rate of appearance of the drug on the receiver side, divided by $A \times 60 \times C_0$, where A is the surface area of the Caco-2 cell monolayer (1.12 cm²) and C_0 is the loading concentration of the drug on the apical side.

2.4. *In Vivo* Pharmacokinetic Study at a Micro-Dose Range

2.4.1. Animal Study

For SFN and SFN-NAC, pharmacokinetics was assessed in male Sprague-Dawley rats (7–8 weeks old, 220–280 g) obtained from Orient Bio Inc. (Seongnam, Korea). Rats were maintained under a standard 12:12 h light/dark cycle for 1 week. All experiments complied with the guidelines for animal care and use issued by Gachon University, and experimental animal protocols were reviewed and approved by the Animal Care and Use Committee of Gachon University (#GIACUC-R2018004, approval date: 11 May 2018).

For the intravenous study, overnight fasted rats were intramuscularly anesthetized using tiletamine/zolazepam (Zoletil; Vibrac Laboratories, Carros, France) (20 mg/kg). Then, the femoral vein and artery were surgically cannulated with polyethylene tubing (PE50; Clay Adams, Parsippany, NJ, USA) for intravenous administration of test compounds and blood sampling, respectively. The cannula was flushed with 20 IU/mL heparinized saline to prevent clotting. After the rats had recovered from anesthesia, SFN or SFN-NAC was injected intravenously at 0.1 mg/kg ($n = 4$). Blood samples (100 μ L) were collected from the femoral artery 1, 5, 15, 30, 45, 60, 120, 180, and 240 min after administration, then immediately centrifuged at 14,000 rpm for 15 min at 4 °C, and the plasma obtained was stored at -70 °C prior to LC-MS/MS analysis. For the oral study, the femoral vein was cannulated for blood sampling, followed by administration of SFN (0.1, 0.2, and 0.5 mg/kg) or SFN-NAC (0.5 mg/kg) using oral gavage. Blood samples (100 μ L) were collected from

the femoral artery 15, 30, 45, 60, 120, 180, 240, 480, and 1440 min after administration and processed in the same way as in the intravenous study.

2.4.2. Pharmacokinetic Analysis

Noncompartmental analysis of SFN and SFN-NAC was performed using the Win-Nonlin program (Ver. 5.0.1., Pharsight Corporation, Mountain View, CA, USA) to calculate the following pharmacokinetic parameters: area under the plasma concentration-time curve from time zero to infinity (AUC_{inf}) or to the last measured time (AUC_{last}), total body clearance (CL), elimination half-life ($t_{1/2}$), volume of distribution at steady-state (V_{ss}), and mean residence time (MRT). The AUC was calculated using the trapezoidal rule extrapolation method. The maximum plasma concentration (C_{max}) and time to reach C_{max} (T_{max}) were directly determined from the experimental data, and the area from the last datum point to time infinity (for the calculation of AUC_{inf}) was estimated by dividing the last measured plasma concentration by the terminal-phase rate constant. The absolute bioavailability (F%) was calculated as the dose-normalized ratio of the AUC after oral and intravenous administration.

2.5. LC-MS/MS Analysis

In the present study, sample concentrations from in vitro or in vivo pharmacokinetic studies were determined using LC-MS/MS in positive electrospray ionization mode. The LC-MS/MS system consisted of an Agilent 6490 QQQ with a 1290 Infinity HPLC system (Agilent Technologies, Santa Clara, CA, USA). To separate the analytes, SFN and SFN-NAC, from endogenous substances, a SynergiTM 4 μ m polar RP 80A column (150 \times 2.0 mm, Phenomenex, Torrance, CA, USA) was employed. The LC conditions were as follows: mobile phase, 0.1% formic acid and acetonitrile (50:50); flow rate, 0.2 mL/min; injection volume, 2 μ L. Multiple reaction monitoring was achieved with m/z 178.1 \rightarrow 114.1 for SFN, m/z 340.9 \rightarrow 178.1 for SFN-NAC, and m/z 176.1 \rightarrow 111.9 for an internal standard (sulforaphene). Data acquisition and processing were performed using the MassHunter software (version A.06.00, Agilent Technologies). The limit of quantitation was 0.2 ng/mL for SFN and 0.5 ng/mL for SFN-NAC.

2.6. Statistical Analyses

Data are expressed as mean \pm standard deviation (SD) of at least three independent experiments. For statistical analysis, one-way analysis of variance (ANOVA) with post-hoc Dunnett's test was performed using GraphPad Prism software (San Diego, CA, USA). p -values less than 0.05 were considered statistically significant.

3. Results

3.1. In Vitro Anti-Fibrosis Effects of SFN and SFN-NAC

We evaluated the effect of SFN and SFN-NAC on lung cell viability. Accordingly, MRC-5 cells were incubated with different concentrations of SFN and SFN-NAC (10 and 20 μ M). At maximal SFN and SFN-NAC concentrations, MRC-5 cells showed no cytotoxicity (Figure 2). The deposition of ECM proteins (FN, COL1A1, and COL4A1) and myofibroblast marker (α -SMA) is considered to be a significant event in tissue remodeling and fibrosis. Therefore, the inhibitory effect of SFN and SFN-NAC on the expression levels of ECM proteins was assessed using qRT-PCR and western blot analyses. In the present study, our findings revealed that the mRNA and protein expression levels of ECM proteins, including FN, α -SMA, COL1A1, and COL1A4, were increased in TGF- β 1-induced fibroblast cells. Conversely, SFN and SFN-NAC treatment significantly decreased TGF- β 1-induced mRNA and protein expression levels in a dose-dependent manner (Figures 3 and 4). Notably, the inhibitory effect of SFN-NAC on FN, α -SMA, and COL1A4 proteins was comparable with that mediated by SFN (Figure 4). However, SFN-NAC induced significant inhibitory effects on COL1A1 proteins; this effect was not demonstrated following the SFN treatment (Figure 4).

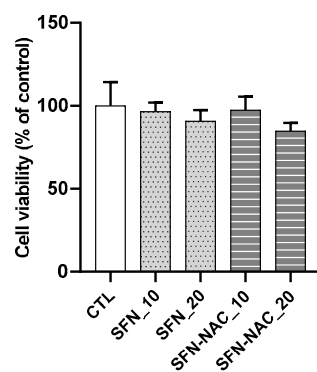


Figure 2. Effect of SFN and SFN-NAC on cell viability of MRC-5 fibroblast cells. The cells were treated with indicated concentrations (10 and 20 μ M) of SFN and SFN-NAC for 48 h. Data values are expressed as the mean \pm standard deviation of at least three different experiments. SFN, sulforaphane; SFN-NAC, sulforaphane *N*-acetylcysteine; CTL, control.

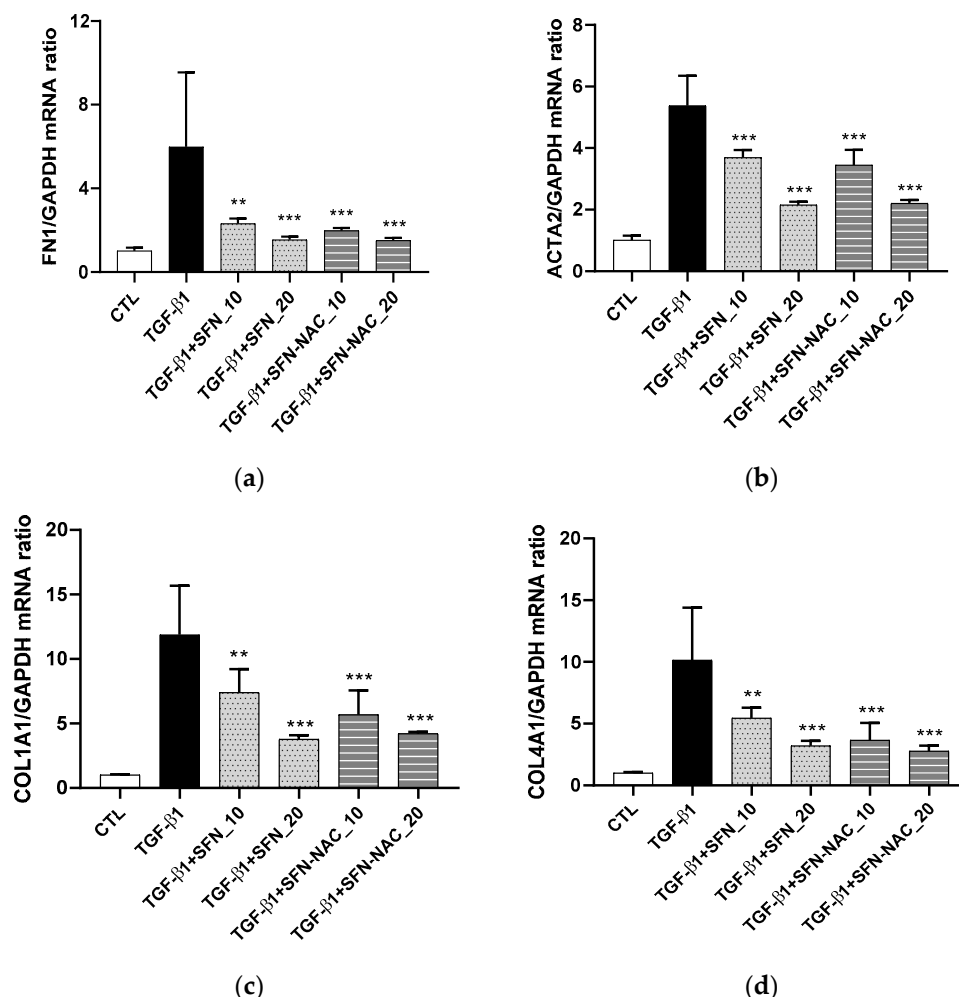


Figure 3. Effect of SFN and SFN-NAC treatment on the mRNA expression of ECM proteins and myofibroblast marker following TGF- β 1-induced fibrosis in MRC-5 fibroblast cells. The cells were pre-treated for 1 h with the indicated concentrations of SFN and SFN-NAC, followed by treatment with TGF- β 1 (5 ng/mL) for 48 h. mRNA levels of *FN1* (a), *ACTA2* (b), *COL1A1* (c), and *COL4A1* (d) were measured by qRT-PCR. Data values are expressed as the mean \pm standard deviation of at least three different experiments. ** $p < 0.01$, *** $p < 0.001$ versus TGF- β 1 induction. ECM, extracellular proteins; TGF- β 1, transforming growth factor- β 1; SFN, sulforaphane; SFN-NAC, sulforaphane *N*-acetylcysteine; CTL, control; *FN1*, fibronectin 1; *ACTA2*, actin alpha2, smooth muscle; *COL1A1*, type I collagen; *COL4A1*, type IV collagen.

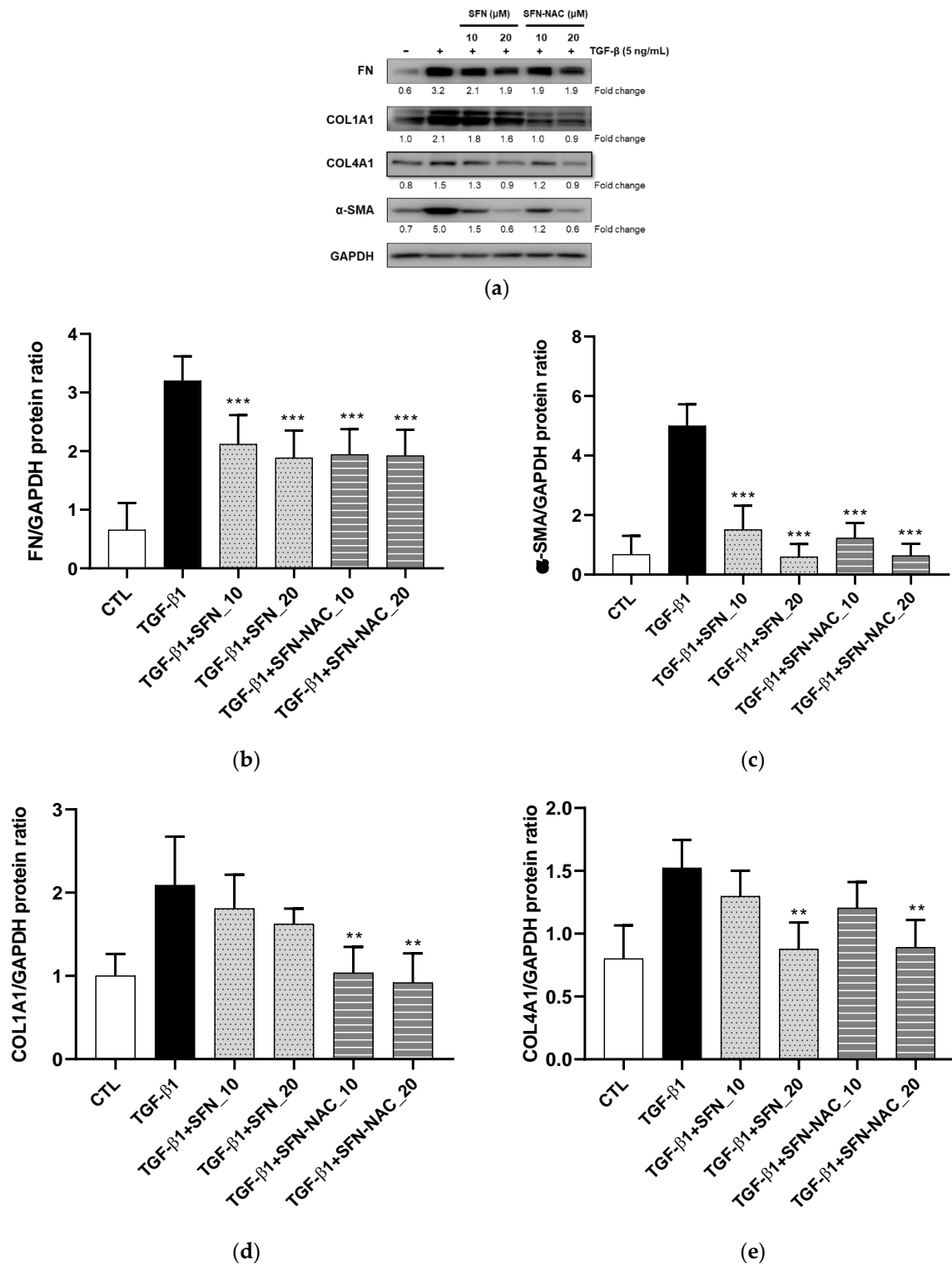


Figure 4. Effect of SFN and SFN-NAC treatment on the expression of ECM proteins and myofibroblast marker following TGF- β 1-induced fibrosis in MRC-5 fibroblast cells. The cells were pre-treated for 1 h with the indicated concentrations of SFN and SFN-NAC, followed by treatment with TGF- β 1 (5 ng/mL) for 48 h. (a) Western blot analysis for FN, α -SMA, COL1A1 and COL4A1. Densitometry of Western blotting of FN (b), α -SMA (c), COL1A1 (d), and COL4A1 (e). Data are expressed as the mean \pm standard deviation of at least three different experiments. ** $p < 0.01$, *** $p < 0.001$ versus TGF- β 1 induction. ECM, extracellular proteins; TGF- β 1, transforming growth factor- β 1; SFN, sulforaphane; SFN-NAC, sulforaphane *N*-acetylcysteine; CTL, control; FN, fibronectin; α -SMA, alpha-smooth muscle actin; COL1A1, type I collagen; COL4A1, type IV collagen.

3.2. In Vitro Pharmacokinetic Properties

3.2.1. Metabolic Stability of SFN and SFN-NAC

SFN levels were reduced in rat and human plasma, presenting mean half-lives of 76.0 and 57.4 min, respectively (Figure 5a,b). The plasma level of SFN-NAC decreased faster than that of SFN, with mean half-lives of 23.3 and 19.0 min, respectively. In both rat and human plasma, SFN was formed after incubation with SFN-NAC. The concentration of the formed SFN increased and then decreased again in a similar manner to that following incubation with SFN (Figure 5c,d).

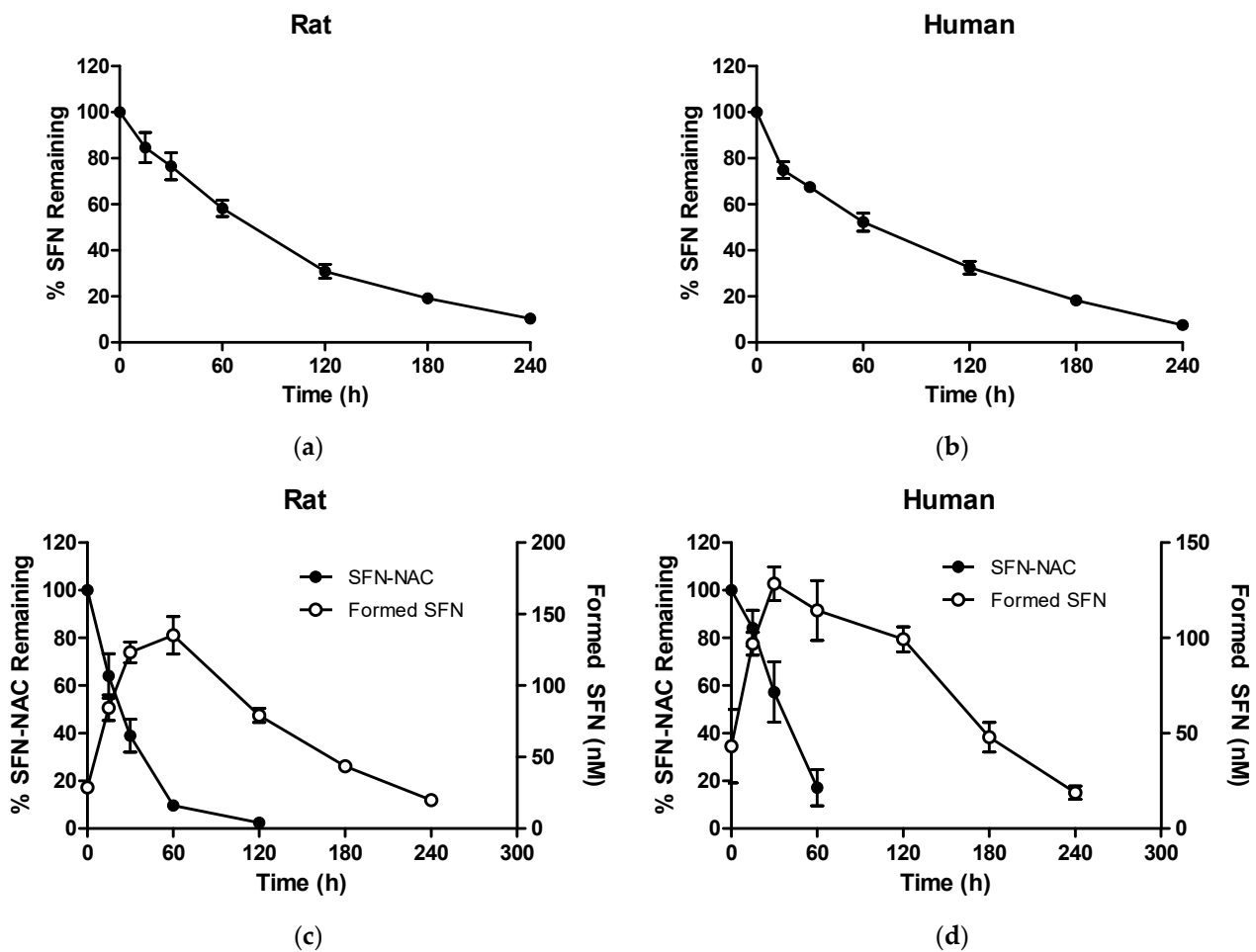


Figure 5. Percentages of remaining SFN and SFN-NAC as a function of time after incubation in plasma: (a) SFN in rat plasma; (b) SFN in human plasma; (c) SFN-NAC in rat plasma; (d) SFN-NAC in human plasma. Data values are expressed as the mean \pm standard deviation ($n = 3$ at each point). SFN, sulforaphane; SFN-NAC, sulforaphane *N*-acetylcysteine.

After liver microsomal incubation for 240 min, the decrease in SFN concentration was substantially more gradual when compared with that in plasma, with 83.7% and 70.3% remaining in rat and human microsomes, respectively (Figure 6c,d). Similarly to in plasma, SFN was formed from SFN-NAC when SFN-NAC was incubated in liver microsomes. However, unlike in plasma, the concentration of formed SFN did not decrease until 240 min, probably due to the slower metabolic rate of SFN in liver microsomes.

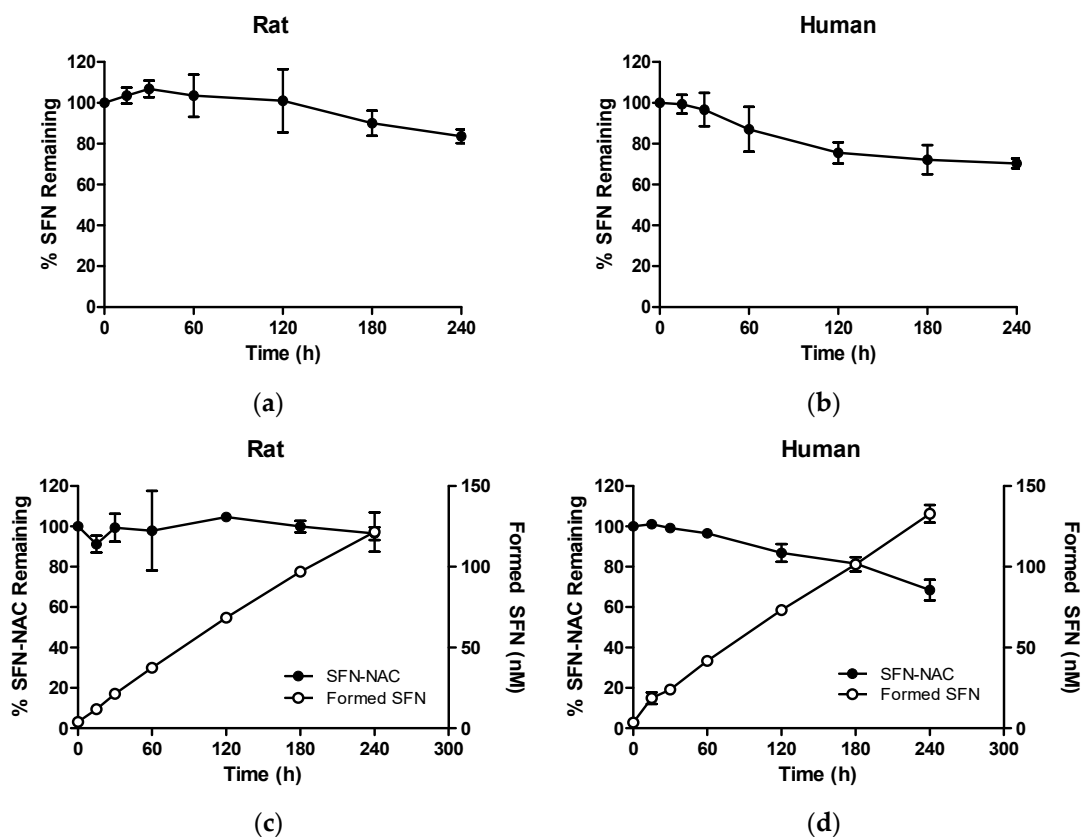


Figure 6. Percentages of SFN and SFN-NAC remaining as a function of time after incubation in liver microsomes: (a) SFN in rat liver microsomes; (b) SFN-NAC in rat liver microsomes; (c) SFN in human liver microsomes; (d) SFN-NAC in human liver microsomes. Data values are expressed as the mean \pm standard deviation ($n = 3$ at each point). SFN, sulforaphane; SFN-NAC, sulforaphane *N*-acetylcysteine.

3.2.2. Apparent Permeability for Absorption Direction in Caco-2 Cells

The apical-to-basolateral transport of SFN and SFN-NAC across Caco-2 monolayers was investigated (Figure 7). Compared to that of SFN, the A-to-B transport of SFN-NAC was much lower. The calculated apparent permeability coefficients ($P_{app, A-to-B}$) of SFN were $1.33 \pm 0.01 \times 10^{-5}$ cm/s, whereas the $P_{app, A-to-B}$ of SFN-NAC was much lower, $0.16 \pm 0.01 \times 10^{-6}$ cm/s, suggesting a much higher intestinal absorption of SFN compared to SFN-NAC in terms of permeability.

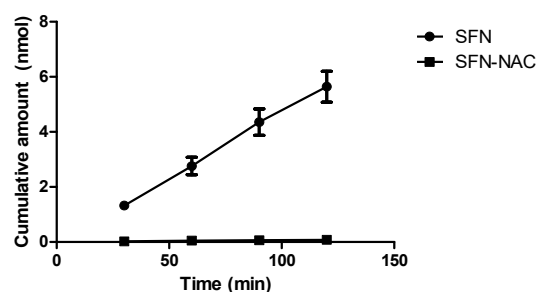


Figure 7. Cumulative amount of SFN and SFN-NAC transported across Caco-2 cell monolayers over time. Data values are expressed as the mean \pm standard deviation ($n = 3$ at each point). SFN, sulforaphane; SFN-NAC, sulforaphane *N*-acetylcysteine.

3.3. In Vivo Pharmacokinetic Study at a Micro-Dose Range

3.3.1. Sulforaphane

After intravenous administration of 0.1 mg/kg SFN, the SFN plasma concentration declined exponentially, with a terminal half-life of 61.3 min (Figure 8a and Table 1). The total body clearance of SFN was 40.7 mL/min/kg. After oral administration of SFN at 0.1, 0.2, and 0.5 mg/kg, the T_{max} ranged between 5–30 min for the three different doses. The increase in the oral AUC of SFN was more than dose-proportional, indicating non-linear pharmacokinetics of SFN even in the low dose range (Figure 8b and Table 1). Thus, the calculated oral bioavailability was similar, between 0.1 mg/kg and 0.2 mg/kg, whereas the oral bioavailability was higher than 100% at the highest dose (0.5 mg/kg).

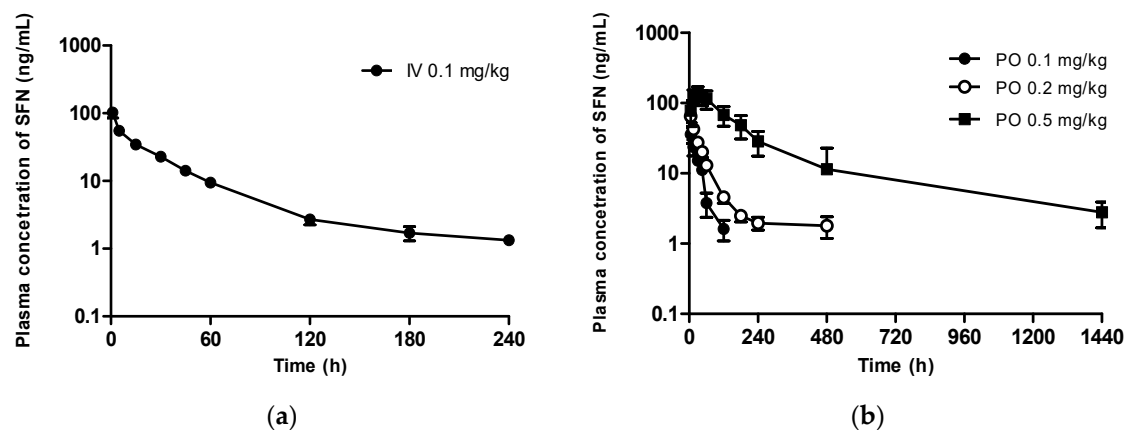


Figure 8. Plasma concentration of SFN after (a) intravenous (0.1 mg/kg) and (b) oral (0.1, 0.2, and 0.5 mg/kg) administration to rats. Data values are expressed as the mean \pm standard deviation ($n = 4$). SFN, sulforaphane.

Table 1. Pharmacokinetic parameters of SFN after intravenous (0.1 mg/kg) and oral (0.1, 0.2, and 0.5 mg/kg) administration to rats. Data values are expressed as the mean \pm standard deviation ($n = 4$).

Parameters	IV		PO	
	0.1 mg/kg	0.1 mg/kg	0.2 mg/kg	0.5 mg/kg
AUC _{last} ($\mu\text{g}\cdot\text{min}/\text{mL}$)	2.35 \pm 0.154	1.85 \pm 0.377	3.16 \pm 0.073	29.8 \pm 8.64
AUC _{inf} ($\mu\text{g}\cdot\text{min}/\text{mL}$)	2.47 \pm 0.205	1.92 \pm 0.411	3.57 \pm 0.253	31.0 \pm 8.89
$t_{1/2}$ (min)	61.3 \pm 36.2	41.9 \pm 7.60	197.7 \pm 169	320 \pm 75.4
MRT (min)	56.2 \pm 11.7			
C_{max} ($\mu\text{g}/\text{mL}$)	-	0.036 \pm 0.010	0.065 \pm 0.012	0.143 \pm 0.035
T_{max} (min)	-	15.0 \pm 0.0	5.0 \pm 0.0	30.0 \pm 18.4
V_{ss} (mL/kg)	2268 \pm 337			
CL (mL/min/kg)	40.7 \pm 3.4			
F (%)		77.8%	72.4%	251.4%

SFN, sulforaphane; IV, intravenous; PO, peroral; AUC_{last}, area under the plasma concentration-time curve from time zero to the last measured time; AUC_{inf}, area under the plasma concentration-time curve from time zero to infinity; $t_{1/2}$, elimination half-life; MRT, mean residence time; C_{max} , maximum serum drug concentration; T_{max} , time take to reach C_{max} ; V_{ss} , volume of distribution at steady-state; CL, total body clearance; F(%), oral bioavailability, i.e., the fraction of an orally administered drug that reaches systemic circulation.

3.3.2. Sulforaphane N-acetylcysteine

After intravenous administration of 0.1 mg/kg SFN-NAC, the plasma concentration of SFN declined exponentially, presenting a terminal half-life of 33.2 min (Figure 9a and Table 2). The total body clearance of SFN-NAC was 48.3 mL/min/kg, similar to that of SFN. The plasma concentration of the formed SFN was determined after administering SFN-NAC. SFN was rapidly formed from SFN-NAC and decreased in a similar pattern and concentration range to SFN-NAC. The half-life of the formed SFN was 48.6 min, which approaches that of SFN after an oral dose of 0.1 mg/kg (Tables 1 and 2).

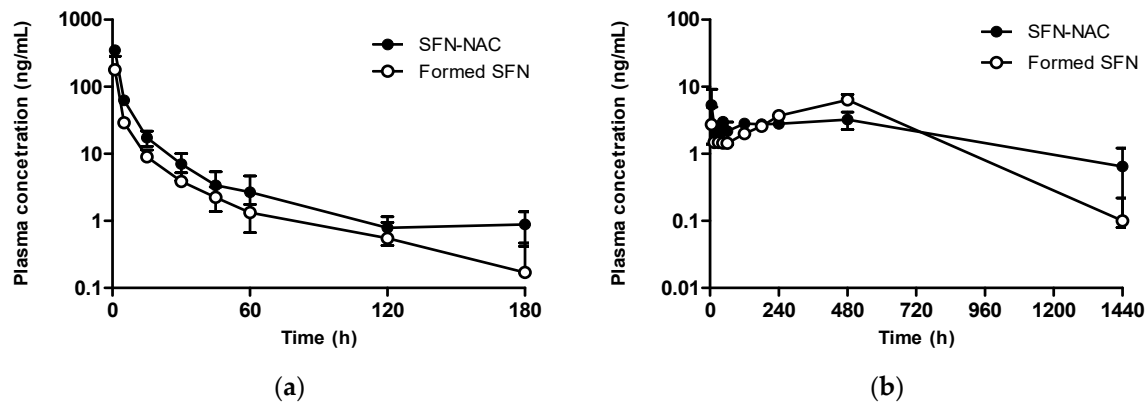


Figure 9. Plasma concentration of SFN-NAC and SFN after (a) intravenous (0.1 mg/kg) and (b) oral (0.5 mg/kg) administration of SFN-NAC to rats. Data values are expressed as means \pm standard deviation ($n = 4$). SFN, sulforaphane; SFN-NAC, sulforaphane *N*-acetylcysteine.

Table 2. Pharmacokinetic parameters of SFN-NAC and SFN after intravenous (0.1 mg/kg) and oral (0.5 mg/kg) administration of SFN-NAC to rats. The data are expressed as the mean \pm standard deviation ($n = 4$).

Parameters	IV (SFN-NAC 0.1 mg/kg)		PO (SFN-NAC 0.5 mg/kg)	
	SFN-NAC	SFN	SFN-NAC	SFN
AUC _{last} ($\mu\text{g}\cdot\text{min}/\text{mL}$)	2.11 \pm 0.502	1.07 \pm 0.215	2.67 \pm 1.22	1.73 \pm 0.186
AUC _{inf} ($\mu\text{g}\cdot\text{min}/\text{mL}$)	2.16 \pm 0.515	1.11 \pm 0.233	NC	NC
$t_{1/2}$ (min)	33.2 \pm 14.2	48.6 \pm 11.0	NC	NC
MRT (min)	15.8 \pm 7.7			
C_{max} ($\mu\text{g}/\text{mL}$)	-		0.006 \pm 0.003	0.006 \pm 0.001
T_{max} (min)	-			
V_{ss} (mL/kg)	711 \pm 262	-	-	-
CL (mL/min/kg)	48.3 \pm 10.5	-	-	-
F(%)	-	-	>24.8%	-

SFN, sulforaphane; SFN-NAC, sulforaphane *N*-acetylcysteine; IV, intravenous; PO, peroral; AUC_{last}, area under the plasma concentration-time curve from time zero to the last measured time; AUC_{inf}, area under the plasma concentration-time curve from time zero to infinity; $t_{1/2}$, elimination half-life; MRT, mean residence time; C_{max} , maximum serum drug concentration; T_{max} , time taken to reach C_{max} ; V_{ss} , volume of distribution at steady-state; CL, total body clearance; F(%), oral bioavailability, i.e., the fraction of an orally administered drug that reaches systemic circulation.

After oral administration of 0.5 mg/kg SFN-NAC, the bioavailability of SFN-NAC (24.8%) was lower than that of SFN (Figure 9b and Table 2). This could be attributed to poor intestinal absorption, as the C_{max} of SFN-NAC was 0.006 $\mu\text{g}/\text{mL}$, while that of SFN was 0.143 $\mu\text{g}/\text{mL}$ at identical doses. Moreover, SFN was formed after the oral administration of SFN-NAC. The concentration of SFN decreased in the early phase and then increased until 8 h after administration.

4. Discussion

SFN and SFN metabolites are known to possess various pharmacological activities. In the present study, our findings first revealed the antifibrotic effects of SFN and SFN-NAC, the major metabolite of SFN. Furthermore, the pharmacokinetic profiles of SFN and SFN-NAC were evaluated to confirm their potential as therapeutic agents for pulmonary fibrosis.

In the present study, we observed that SFN and SFN-NAC inhibited TGF- β 1-induced fibrosis in pulmonary fibroblasts. Both SFN and SFN-NAC significantly inhibited the overexpression of fibrosis-related proteins, including FN, α -SMA, COL1A1, and COL4A1, induced by TGF- β 1 in fibroblast cells without observed cytotoxicity (Figures 3 and 4). TGF- β , a potent fibrotic mediator, acts on multiple cell types during fibrosis, inducing fibroblast proliferation and differentiation into myofibroblasts [25–27]. In addition, the mRNA expres-

sion of these proteins was decreased following SFN and SFN-NAC treatment. FN, α -SMA, and collagens are major fibrous proteins that compose the ECM and play crucial roles in cell adhesion, including differentiation, growth, migration, and wound healing [28]. Excessive deposition contributes to the pathogenesis of pulmonary fibrosis [25,28]. Both SFN and SFN-NAC presented similar inhibitory effects mediated by anti-pulmonary fibrosis-related genes (Figures 3 and 4), suggesting that the antifibrotic effect could be sustained even after SFN metabolism to SFN-NAC, the final major metabolite, by administering SFN-containing food or SFN itself.

Therefore, to accurately understand the pharmacological effects of SFN and SFN-NAC, we evaluated the pharmacokinetics of both SFN and SFN-NAC. Both SFN and SFN-NAC were stable during liver metabolism, but their concentration rapidly decreased in the plasma, indicating that the rapid clearance of SFN might be due to plasma metabolism. The volume of distribution of SFN was moderate, implying that SFN could be distributed to target tissues such as the lung and liver to exhibit antifibrotic effects. Following oral administration, the bioavailability was over 70%; sufficient for development as a therapeutic agent. As large variabilities in pharmacokinetic parameters of SFN have been reported in previous studies, we evaluated the pharmacokinetics of SFN at low doses, ranging from 0.1 to 0.5 mg/kg. The pharmacokinetic parameters of SFN presented linear kinetics up to 0.2 mg/kg; however, at 0.5 mg/kg, the drug exposure exceeded the proportional dose (Table 1), which could be attributed to the saturable metabolism of SFN and/or re-conversion of SFN-NAC to SFN. Notably, in the high dose range assessed in a previous pharmacokinetic study, the dose-normalized AUC and SFN bioavailability decreased in the range of 0.5 to 5 mg/kg, possibly due to saturation of the absorption process [21]. After intravenous and oral administration of SFN-NAC, rapid formation of SFN was confirmed with a similar decrease in SFN, indicating rapid equilibrium in the reversible metabolism between SFN and SFN-NAC.

Despite its various therapeutic benefits, SFN presents several problems that need to be resolved prior to oral administration. Broccoli sprout extracts containing glucosinolates (the precursor of SFN) and SFN have shown good tolerability and no significant side effects in humans [29]. However, gastrointestinal side effects such as bloating, diarrhea, dyspepsia, and flatulence have been observed on administering a large SFN dose [30]. Furthermore, Lozanovski et al. have reported that broccoli sprouts can cause digestive issues, such as vomiting and nausea [31]. In terms of pharmacokinetics, as SFN itself is unstable, it is difficult to maintain an efficacious concentration for a sufficient period. Based on the finding that SFN-NAC is converted to SFN, an SFN-NAC prodrug could be an alternative approach to overcome the above challenges, although SFN-NAC is also a major metabolite of SFN. Notably, it was first demonstrated that SFN could be formed from SFN-NAC in plasma and liver microsomal stability studies, possibly due to the deconjugation reaction (Figures 5 and 6). Moreover, upon SFN-NAC administration via intravenous or oral administration, the formed SFN was rapidly converted and maintained in vivo along with SFN-NAC. However, the absolute oral bioavailability of SFN-NAC was found to be low (>24.8%) when compared with that following SFN administration (Tables 1 and 2), indicating that chemical modification is crucial for enhancing intestinal absorption when developing SFN-NAC as a novel drug candidate. Moreover, considering that SFN-NAC, the major SFN metabolite, undergoes gastrointestinal absorption after conversion to SFN-NAC, the reversible metabolism between SFN-NAC and SFN could lead to long-term pharmacological effects, as afforded by antifibrotic agents in the lungs.

5. Conclusions

The anti-pulmonary fibrotic effects, as well as the in vitro and in vivo pharmacokinetics of SFN and SFN-NAC, a major metabolite of SFN, were evaluated to elucidate the effects of SFN-containing products. Our findings revealed that SFN and SFN-NAC present similar antifibrotic activities. Furthermore, as SFN-NAC is reconverted to SFN in the body, SFN-NAC can be potentially developed as an alternative to overcome the gastrointestinal

side effects associated with SFN. If the low absorption of SFN-NAC can be improved by chemical modification in the future, SFN-NAC could be a promising therapeutic agent to achieve a prolonged duration of action, with reduced side effects of SFN and its metabolites.

Author Contributions: Conceptualization, S.H.J. and Y.C.K.; methodology, E.S.S., X.F. and J.-H.Y.; software, J.-H.Y.; formal analysis, E.S.S. and J.-H.Y.; investigation, E.S.S. and J.-H.Y.; resources, X.F. and S.-Y.S.; data curation, E.S.S. and H.-J.M.; writing—original draft preparation, E.S.S., X.F., H.-J.M. and Y.C.K.; writing—review and editing, H.-J.M., S.H.J. and Y.C.K.; visualization, E.S.S., X.F. and S.-Y.S.; supervision, S.H.J. and Y.C.K.; project administration, S.H.J.; funding acquisition, H.-J.M. and S.H.J. All authors have read and agreed to the published version of the manuscript.

Funding: This research was funded by the Basic Science Research Program through the National Research Foundation of Korea (NRF), funded by the Ministry of Science, ICT & Future Planning (grant numbers NRF-2018R1A6A3A11047142, 20191A2C2089867, 2019R1F1A1058103, and 2020R1C1C1008148).

Institutional Review Board Statement: The study was conducted according to the Guide for the Care and Use of Laboratory Animals issued by the National Institute of Health, and approved by the Animal Care and Use Committee of Gachon University (GIACUC-R2018004, approval date: 11 May 2018).

Informed Consent Statement: Not applicable.

Data Availability Statement: The data presented in this study are available in the article.

Conflicts of Interest: The authors declare no conflict of interest. The funders had no role in the design of the study; in the collection, analyses, or interpretation of data; in the writing of the manuscript, or in the decision to publish the results.

References

1. Li, H.; Zhao, C.; Tian, Y.; Lu, J.; Zhang, G.; Liang, S.; Chen, D.; Liu, X.; Kuang, W.; Zhu, M. Src family kinases and pulmonary fibrosis: A review. *Biomed. Pharmacother.* **2020**, *127*, 110183. [[CrossRef](#)]
2. Liu, P.; Miao, K.; Zhang, L.; Mou, Y.; Xu, Y.; Xiong, W.; Yu, J.; Wang, Y. Curdione ameliorates bleomycin-induced pulmonary fibrosis by repressing TGF- β -induced fibroblast to myofibroblast differentiation. *Respir. Res.* **2020**, *21*, 58. [[CrossRef](#)]
3. Phan, S.H. The myofibroblast in pulmonary fibrosis. *Chest* **2002**, *122*, 286S–289S. [[CrossRef](#)] [[PubMed](#)]
4. Park, S.D.; Jung, J.H.; Lee, H.W.; Kwon, Y.M.; Chung, K.H.; Kim, M.G.; Kim, C.H. Zedoariae rhizoma and curcumin inhibits platelet-derived growth factor-induced proliferation of human hepatic myofibroblasts. *Int. Immunopharmacol.* **2005**, *5*, 555–569. [[CrossRef](#)] [[PubMed](#)]
5. Fenwick, G.R.; Heaney, R.K. Glucosinolates and their breakdown products in cruciferous crops, foods and feeding stuffs. *Food Chem.* **1983**, *11*, 249–271. [[CrossRef](#)]
6. Wattenberg, L.W. Inhibition of carcinogenic effects of polycyclic hydrocarbons by benzyl isothiocyanate and related compounds. *J. Natl. Cancer Inst.* **1977**, *58*, 395–398. [[CrossRef](#)] [[PubMed](#)]
7. Hecht, S.S. Chemoprevention of isothiocyanates. *J. Cell. Biochem. Suppl.* **1995**, *22*, 195–209. [[CrossRef](#)]
8. Chung, E.L. Chemoprevention of lung cancer by isothiocyanates and their conjugates in A/J mouse. *Exp. Lung Res.* **2001**, *27*, 319–330. [[CrossRef](#)]
9. Conaway, C.C.; Wang, C.X.; Pittman, B.; Yang, Y.M.; Schwartz, J.E.; Tian, D.; McIntee, E.J.; Hecht, S.S.; Chung, F.L. Phenethyl isothiocyanate and sulforaphane and their N-acetylcysteine conjugates inhibit malignant progression of lung adenomas induced by tobacco carcinogens in A/J mice. *Cancer Res.* **2005**, *65*, 8548–8557. [[CrossRef](#)]
10. Kan, S.F.; Wang, J.; Sun, G.X. Sulforaphane regulates apoptosis- and proliferation-related signaling pathways and synergizes with cisplatin to suppress human ovarian cancer. *Int. J. Mol. Med.* **2018**, *42*, 2447–2458. [[CrossRef](#)]
11. Yang, Y.M.; Conaway, C.C.; Chiao, J.W.; Wang, C.X.; Amin, S.; Whysner, J.; Dai, W.; Reinhardt, J.; Chung, F.L. Inhibition of benzo(a)pyrene-induced lung tumorigenesis in A/J mice by dietary N-acetylcysteine conjugates of benzyl and phenethyl isothiocyanates during the post-initiation phase is associated with activation of MAP kinases and p53 activity and induction of apoptosis. *Cancer Res.* **2002**, *62*, 2–7.
12. Kyung, S.Y.; Kim, D.Y.; Yoon, J.Y.; Son, E.S.; Kim, Y.J.; Park, J.W.; Jeong, S.H. Sulforaphane attenuates pulmonary fibrosis by inhibiting the epithelial-mesenchymal transition. *BMC Pharmacol. Toxicol.* **2018**, *19*, 13. [[CrossRef](#)]
13. Conaway, C.C.; Getahun, S.M.; Liebes, L.L.; Pusateri, D.J.; Topham, D.K.; Botero-Omary, M.; Chung, F.L. Disposition of glucosinolates and sulforaphane in humans after ingestion of steamed and fresh broccoli. *Nutr. Cancer* **2000**, *38*, 168–178. [[CrossRef](#)]

14. Gasper, A.V.; Al-Janobi, A.; Smith, J.A.; Bacon, J.R.; Fortun, P.; Atherton, C.; Taylor, M.A.; Hawkey, C.J.; Barrett, D.A.; Mithen, R.F. Glutathione S-transferase M1 polymorphism and metabolism of sulforaphane from standard and high-glucosinolate broccoli. *Am. J. Clin. Nutr.* **2005**, *82*, 1283–1291. [[CrossRef](#)]
15. Mennicke, W.H.; Gorler, K.; Krumbiegel, G.; Lorenz, D.; Rittmann, N. Studies on the metabolism and excretion of benzyl isothiocyanate in man. *Xenobiotica* **1988**, *82*, 39–47. [[CrossRef](#)]
16. Jiao, D.; Ho, C.T.; Fioles, P.; Chung, F.L. Identification and quantification of the *N*-acetylcysteine conjugate of allyl isothiocyanate in human urine after ingestion of mustard. *Cancer Epidemiol. Biomarkers Prev.* **1994**, *3*, 487–492.
17. Tang, L.; Li, G.; Song, L.; Zhang, Y. The principal urinary metabolites of dietary isothiocyanates, *N*-acetylcysteine conjugates, elicit the same anti-proliferative response as their parent compounds in human bladder cancer cells. *Anticancer Drugs* **2006**, *17*, 297–305. [[CrossRef](#)]
18. Zhou, Y.; Yang, G.; Tian, H.; Hu, Y.; Wu, S.; Geng, Y.; Lin, K.; Wu, W. Sulforaphane metabolites cause apoptosis via microtubule disruption in cancer. *Endocr. Relat. Cancer* **2018**, *25*, 255–268. [[CrossRef](#)]
19. Mitsiogianni, M.; Koutsidis, G.; Mavroudis, N.; Trafalis, D.T.; Botaitis, S.; Franco, R.; Zoumpourlis, V.; Amery, T.; Galanis, A.; Pappa, A.; et al. The role of isothiocyanates as cancer chemo-preventive, chemo-therapeutic and anti-melanoma agents. *Antioxidants* **2019**, *8*, 106. [[CrossRef](#)]
20. Hu, R.; Hebbar, V.; Kim, B.R.; Chen, C.; Winnik, B.; Buckley, B.; Soteropoulos, P.; Toliass, P.; Hart, R.P.; Kong, A.N. In vivo pharmacokinetics and regulation of gene expression profiles by isothiocyanate sulforaphane in the rat. *J. Pharmacol. Exp. Ther.* **2004**, *310*, 263–271. [[CrossRef](#)]
21. Hanlon, N.; Coldham, N.; Gielbert, A.; Kuhnert, N.; Sauer, M.J.; King, L.J. Ioannides C Absolute bioavailability and dose-dependent pharmacokinetic behaviour of dietary doses of the chemopreventive isothiocyanate sulforaphane in rat. *Br. J. Nutr.* **2008**, *99*, 559–564. [[CrossRef](#)]
22. Wang, H.; Khor, T.O.; Yang, Q.; Huang, Y.; Wu, T.Y.; Saw, C.L.; Lin, W.; Androulakis, I.P.; Kong, A.N. Pharmacokinetics and pharmacodynamics of phase II drug metabolizing/antioxidant enzymes gene response by anticancer agent sulforaphane in rat lymphocytes. *Mol. Pharm.* **2012**, *9*, 2819–2827. [[CrossRef](#)]
23. Doan, T.N.K.; Vo, D.K.; Kim, H.; Balla, A.; Lee, Y.; Yoon, I.S.; Maeng, H.J. Differential effects of 1 α ,25-dihydroxyvitamin D3 on the expressions and functions of hepatic CYP and UGT enzymes and its pharmacokinetic consequences in vivo. *Pharmaceutics* **2020**, *12*, 1129. [[CrossRef](#)]
24. Maeng, H.J.; Chapy, H.; Zaman, S.; Pang, K.S. Effects of 1 α ,25-dihydroxyvitamin D3 on transport and metabolism of adefovir dipivoxil and its metabolites in Caco-2 cells. *Eur. J. Pharm. Sci.* **2012**, *46*, 149–166. [[CrossRef](#)]
25. Selman, M.; King, T.E.; Pardo, A. Idiopathic pulmonary fibrosis: Prevailing and evolving hypotheses about its pathogenesis and implications for therapy. *Ann. Intern. Med.* **2001**, *134*, 136–151. [[CrossRef](#)]
26. Willis, B.C.; Liebler, J.M.; Luby-Phelps, K.; Nicholson, A.G.; Crandall, E.D.; du Bois, R.M.; Borok, Z. Induction of epithelial-mesenchymal transition in alveolar epithelial cells by transforming growth factor-beta1: Potential role in idiopathic pulmonary fibrosis. *Am. J. Pathol.* **2005**, *166*, 1321–1332. [[CrossRef](#)]
27. Richeldi, L.; Collard, H.R.; Jones, M.G. Idiopathic pulmonary fibrosis. *Lancet* **2017**, *389*, 1941–1952. [[CrossRef](#)]
28. Nakamura, T.; Matsushima, M.; Hayashi, Y.; Shibasaki, M.; Imaizumi, K.; Hashimoto, N.; Shimokata, K.; Hasegawa, Y.; Kawabe, T. Attenuation of transforming growth factor- β -stimulated collagen production in fibroblasts by quercetin-induced heme oxygenase-1. *Am. J. Respir. Cell Mol. Biol.* **2011**, *44*, 614–620. [[CrossRef](#)]
29. Shapiro, T.A.; Fahey, J.W.; Dinkova-Kostova, A.T.; Holtzclaw, W.D.; Stephenson, K.K.; Wade, K.L.; Ye, L.; Talalay, P. Safety, tolerance, and metabolism of broccoli sprout glucosinolates and isothiocyanates: A clinical phase I study. *Nutr. Cancer* **2006**, *55*, 53–62. [[CrossRef](#)] [[PubMed](#)]
30. Alumkal, J.J.; Slottke, R.; Schwartzman, J.; Cherala, G.; Munar, M.; Graff, J.N.; Beer, T.M.; Ryan, C.W.; Koop, D.R.; Gibbs, A.; et al. A phase II study of sulforaphane-rich broccoli sprout extracts in men with recurrent prostate cancer. *Investig. New Drugs* **2015**, *33*, 480–489. [[CrossRef](#)]
31. Lozanovski, V.J.; Polychronidis, G.; Gross, W.; Gharabaghi, N.; Mehrabi, A.; Hackert, T.; Schemmer, P.; Herr, I. Broccoli sprout supplementation in patients with advanced pancreatic cancer is difficult despite positive effects—results from the POWDER pilot study. *Investig. New Drugs* **2020**, *38*, 776–784. [[CrossRef](#)] [[PubMed](#)]